THE
EMBO
JOURNAL

Dissection of the unusual structural and functional properties of the variant H2A.Bbd nucleosome

Cécile-Marie Doyen[1,2], Fabien Montel[2,3], Thierry Gautier[1], Hervé Menoni[2,4], Cyril Claudet[5], Marlène Delacour-Larose[1], Dimitri Angelov[2,4], Ali Hamiche[6], Jan Bednar[5,7], Cendrine Faivre-Moskalenko[2,3], Philippe Bouvet[2,4,*] and Stefan Dimitrov[1,2,*]

[1]Institut Albert Bonniot, INSERM U309, La Tronche cedex, France, [2]Laboratoire Joliot-Curie, Ecole Normale Supérieure de Lyon, France, [3]Laboratoire de Physique, CNRS UMR 5672, Ecole Normale Supérieure de Lyon, Lyon, France, [4]Laboratoire de Biologie Moléculaire de la Cellule, CNRS-UMR 5161/INRA 1237/IFR128 Biosciences, Ecole Normale Supérieure de Lyon, Lyon, France, [5]CNRS, Laboratoire de Spectrometrie Physique, UMR 5588, St Martin d'Heres Cedex, France and [6]Institut André Lwoff, CNRS UPR 9079, Villejuif, France

The histone variant H2A.Bbd appeared to be associated with active chromatin, but how it functions is unknown. We have dissected the properties of nucleosome containing H2A.Bbd. Atomic force microscopy (AFM) and electron cryo-microscopy (cryo-EM) showed that the H2A.Bbd histone octamer organizes only ∼130 bp of DNA, suggesting that 10 bp of each end of nucleosomal DNA are released from the octamer. In agreement with this, the entry/exit angle of the nucleosomal DNA ends formed an angle close to 180° and the physico-chemical analysis pointed to a lower stability of the variant particle. Reconstitution of nucleosomes with swapped-tail mutants demonstrated that the N-terminus of H2A.Bbd has no impact on the nucleosome properties. AFM, cryo-EM and chromatin remodeling experiments showed that the overall structure and stability of the particle, but not its property to interfere with the SWI/SNF induced remodeling, were determined to a considerable extent by the H2A.Bbd docking domain. These data show that the whole H2A.Bbd histone fold domain is responsible for the unusual properties of the H2A.Bbd nucleosome.

*Corresponding authors. P Bouvet, Laboratoire de Biologie Moléculaire de la Cellule, CNRS-UMR 5161/INRA 1237/IFR128 Biosciences, Ecole Normale Supérieure de Lyon, 46 Allée d'Italie, 69007 Lyon, France. Tel./Fax: + 33 4 72 72 8016; E-mail: pbouvet@ens-lyon.fr or S Dimitrov, Tel.: + 33 4 76 54 94 73; Fax: + 33 4 76 54 95 95; E-mail: stefan.dimitrov@ujf-grenoble.fr
[7]Present address: Department of Cell Biology, Institute of Physiology, Academy of Sciences of the Czech Republic and Institute of Cellular Biology and Pathology, First Faculty of Medicine, Charles University in Prague, Albertov 4, 128 01 Prague 2, Czech Republic

Received: 28 April 2006; accepted: 31 July 2006; published online: 7 September 2006

Introduction

DNA is packaged into chromatin in the cell nucleus. The chromatin exhibits repeating structure and the repeating unit, the nucleosome, consists of an octamer of the core histones (two each of H2A, H2B, H3 and H4) around which two superhelical turns of DNA are wrapped (van Holde, 1988). The nucleosome presents an obstacle for the protein factors to bind to their cognate DNA sequences and interferes with several vital cellular processes (Beato and Eisfeld, 1997). Histone modifications, ATP-remodeling machines and the incorporation of histone variants within chromatin are used by the cell to overcome the nucleosomal obstacle (Strahl and Allis, 2000; Becker, 2002; Henikoff *et al*, 2004; Henikoff and Ahmad, 2005).

Histone variants are nonallelic isoforms of the conventional histones (van Holde, 1988; Tsanev *et al*, 1993). The function of the different histone variants is poorly understood, but the emerging general picture suggests that the incorporation of histone variants within the nucleosome results in a particle with novel structural and functional properties (Suto *et al*, 2000; Abbott *et al*, 2001; Angelov *et al*, 2003; Bao *et al*, 2004; Gautier *et al*, 2004). The presence of histone variants in the nucleosome has serious impact on several processes, including transcription, repair, cell division and meiosis, and may result in important epigenetic consequences (Ahmad and Henikoff, 2002; Ausio and Abbott, 2002; Kamakaka and Biggins, 2005; Sarma and Reinberg, 2005).

The histone H2A has the largest family of identified variants (Redon *et al*, 2002; Sarma and Reinberg, 2005). This could reflect both the more labile interaction of the H2A–H2B dimer with the remaining histones and DNA (van Holde, 1988) and its strategic position within the core particle (Luger *et al*, 1997). The variants of the H2A family include H2A.X, H2A.Z, macroH2A and H2A.Bbd. H2A.Z and H2A.X are the best studied H2A histone variants to date. H2A.Z is highly conserved, suggesting an important function of this protein (Redon *et al*, 2002). The mammalian H2A.Z is encoded by an essential gene, as its knockout results in embryonic lethality (Faast *et al*, 2001). H2A.Z is involved in both gene activation (Santisteban *et al*, 2000) and gene silencing (Dhillon and Kamakaka, 2000). H2A.Z is also important for chromosome segregation (Rangasamy *et al*, 2004).

H2AX is intimately related to repair. Double strands breaks (DSBs) induce the phosphorylation of H2AX at its C-terminus and this is mediated by members of the PIKK protein family (Rogakou *et al*, 1998). Experiments with H2AX$^{-/-}$ deficient mice showed that H2AX assists the prevention of aberrant repair of DSBs and functions as suppressor of genomic instability and tumors (Bassing *et al*, 2003; Celeste *et al*, 2003).

MacroH2A (mH2A) is an unusual histone variant with a size three-fold of the conventional H2A (Pehrson and Fried,

1992). Immunofluorescence data have shown that the inactive chromosome X is enriched of mH2A (Costanzi and Pehrson, 1998; Mermoud *et al*, 1999; Chadwick *et al*, 2001; Costanzi and Pehrson, 2001). The incorporation of mH2A within the nucleosome interfered with both transcription factor binding and nucleosome remodeling (Angelov *et al*, 2003). *In vitro* and transient transfection experiments showed that mH2A inhibited initiation of transcription and histone acetylation (Perche *et al*, 2000; Doyen *et al*, 2006). It was recently reported that the macrodomain is an ADP-ribose binding module, suggesting that mH2A might also be involved in the biology of ADP-ribose (Karras *et al*, 2005; Kustatscher *et al*, 2005).

H2A.Bbd (B̲arr b̲ody d̲eficient) is the least studied histone variant and microscopy data showed that it is largely excluded from the inactive X chromosome (Chadwick and Willard, 2001; Chadwick *et al*, 2001). This histone variant is quite divergent and its primary sequence showed only 48% identity to its conventional H2A counterpart (Chadwick and Willard, 2001). The N-terminus of H2A.Bbd exhibits a row of six arginines, which could be important for its function. In addition, H2A.Bbd is relatively shorter and lacks both the typical C-terminus of the H2A family and the very last sequence of the docking domain (Chadwick and Willard, 2001; Bao *et al*, 2004). Microccocal nuclease digestion suggested that the H2A.Bbd octamer organized only 118 bp of DNA (Bao *et al*, 2004). FRAP, FRET and sedimentation measurements point to a less stable structure of the variant H2A.Bbd nucleosome (Angelov *et al*, 2004; Bao *et al*, 2004; Gautier *et al*, 2004). The current view is that H2A.Bbd is enriched in nucleosomes associated with transcriptionally active regions of the genome (Chadwick and Willard, 2001) and *in vitro* experiments demonstrated that acetylation of histones contained in H2A.Bbd nucleosomal arrays is facilitated and that these chromatin templates are better transcribed (Angelov *et al*, 2004). The role of the different domains of H2A.Bbd in these processes is not known.

In this work, we report a detailed analysis of the properties of the H2A.Bbd nucleosomes in solution. We have dissected the role of the different domains of H2A.Bbd in the structure and function of H2A.Bbd nucleosomes using a number of physical methods including atomic force microscopy (AFM), electron cryo-microscopy (cryo-EM) and optical tweezers combined with molecular biology approaches. We showed that the H2A.Bbd octamer organizes 130 bp of DNA and that its structural and functional properties are determined by the whole histone fold domain of H2A.Bbd.

Results

### 130 base pairs of DNA are wrapped around the histone variant H2A.Bbd octamer

First we analyzed the structure of the H2A.Bbd particle in solution using microccocal nuclease. Microccocal nuclease digestion measures the accessibility of nucleosomal DNA that is not protected by the histone octamer. To better characterize this accessibility, we performed kinetics studies of the microccocal nuclease digestion of conventional H2A and H2A.Bbd particles reconstituted on the 601 positioning sequence (Figure 1A). The digestion pattern of the conventional particle showed discrete kinetics intermediates at about 208, 160, 146 and 128 bp, whereas the kinetics intermediates of the

H2A.Bbd particle were observed mainly at about 146, 128, 118 and 110 bp. The band at 160 bp, generated upon digestion of the conventional nucleosome, was attributed to the interaction of the N-terminal histone tails with nucleosomal DNA (van Holde, 1980), the 146 bp band represents the core particle, whereas the 128 bp band reflects a subnucleosomal digestion (van Holde, 1980). The origin of the 208 bp band is unknown, but it might be associated with the presence of histones on DNA, as upon digestion of naked 601 DNA, no such band was observed (data not shown). The presence of a faint 160 bp band in the digestion pattern of the H2A.Bbd nucleosome suggests that the interactions of the histone N-termini with DNA were perturbed. The relatively fast disappearance of the 146 bp band in the kinetics of microccocal nuclease digestion suggests a weaker interaction of the 146 bp DNA with the variant histone octamer. Remarkably, the band at 128 bp was less accessible to microccocal nuclease cleavage and was prominent even at 10 min digestion (the latest time point of digestion). This evidences for a strong interaction of the 128 bp DNA with the histone octamer in the H2A.Bbd particle. Finally, the appearance of bands with molecular mass of 118 bp and below in the digestion profile of the variant H2A.Bbd particle only (Figure 1A, see the scans) indicates that the protection against microccocal nuclease digestion is weaker in the variant particle, suggesting a more relaxed structure.

Next, we used microscopy techniques to measure the length of DNA, which is wrapped around the histone octamer. Briefly, using purified recombinant histones we reconstituted both conventional and variant H2A.Bbd centrally positioned nucleosomes on a 255 bp DNA fragment containing the 601 positioning sequence. Initially, AFM was used to visualize the reconstituted particles (Figure 1B–D). The large free DNA sequences present at each end of the nucleosomes allowed the precise measurement of the length of DNA, which is nonwrapped around the histone octamer, and therefore the determination of the length of the DNA organized by the histone octamer. The measurements were carried out on a large number of particles (458 conventional and 290 H2A.Bbd particles), which made the experiment statistically relevant. The mean of distribution of the length of DNA, organized by conventional octamer (Figure 1D) peaked at 146 ± 1.3 bp, in perfect agreement with the crystal structure of the nucleosome (Luger *et al*, 1997). In contrast, the mean length of DNA organized by the octamer containing H2A.Bbd (Figure 1D) peaked at 127 ± 2.2 bp.

The AFM experiment could be affected by the deposition of the material on the functionalized mica surface and by the fact that the measurements were carried out in air. To overcome these potential problems these experiments were repeated, but using cryo-EM. Indeed, cryo-EM measurements carried out in vitrified solution provide high-resolution images of the conformation of the studied samples and were successfully used to study both the nucleosome and the 30 nm chromatin fiber structures (Bednar *et al*, 1995; Bednar and Woodcock, 1999). The electron micrographs clearly showed that the conventional and the variant H2A.Bbd particles exhibit different conformations (Figure 2A and B). The majority of the entry and exit DNA ends of the conventional nucleosomes formed a V-type structure with the nucleosome particle located at the middle of the structure (Figure 2A). In contrast, only a small number of the H2A.Bbd

particles exhibited such structure, whereas the majority of the DNA nucleosomal ends formed an angle close to 180° (Figure 2B). This suggests that the H2A.Bbd octamer interacts weakly with the entry/exit nucleosomal DNA and it is unable to generate a stable V-type orientation to the free DNA ends. The length of the DNA wrapped around the conventional histone octamer was 148 ± 1.9 and 132 ± 2.6 bp for the variant H2A.Bbd octamer (Figure 2C), which is in complete agreement with the AFM measurements. Thus, using two different microscopy techniques we found that H2A.Bbd octamer organizes only 130 bp of DNA. Taken together these results and the microccocal nuclease digestion data, point to a distinct structure of the H2A.Bbd nucleosome with altered interactions of the variant octamer with the nucleosomal DNA.
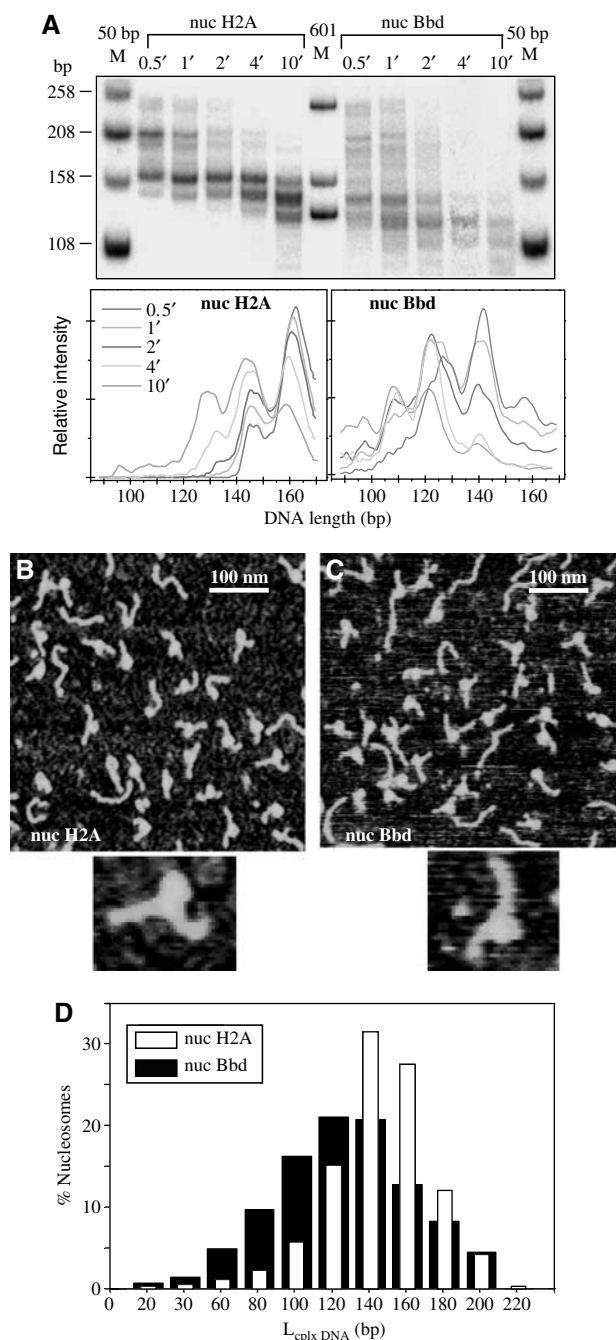
Force–extension measurements of a single H2A.Bbd nucleosomal array

These as well as previous experiments (Bao *et al*, 2004; Gautier *et al*, 2004) suggest that the H2A.Bbd nucleosome exhibits lower stability compared to the conventional nucleosomes, but no direct measurements of the forces maintaining the structure of the H2A.Bbd particle were reported. We addressed this problem using optical tweezers and measured the force necessary for the unfolding of a single H2A.Bbd nucleosome. A fragment of DNA, containing 12 208 bp repeats comprising the 5S rRNA sea urchin gene nucleosome positioning sequence, was used to reconstitute H2A.Bbd nucleosome arrays. Upon digestion of the reconstituted arrays a clear ~ 200 bp repeat was observed indicating a proper organization of the reconstituted samples (data not shown). A single array was then attached between two polysterene beads and subjected to traction using optical tweezers (for details see Materials and methods and Claudet *et al*, 2005). Each small peak in the saw tooth profile of the force–extension curve (Figure 3A) reflects the unfolding of a single H2A.Bbd particle, whereas larger peaks reflect simultaneous unfolding of two nucleosomes (Claudet *et al*, 2005). The same experiment was carried out, but using conventional H2A arrays (results not shown and Claudet *et al*, 2005). The measurements showed that the force necessary for the disruption of a single H2A.Bbd nucleosome was 16.1 ± 4.8 pN, which was very close to the force required for the disruption of a single conventional H2A particle $(17.8 \pm 5.3$ pN) (Figure 3B). The two sets of values of threshold disruption forces were compared using standard *t*-test for two independent populations. The resulting values of *P* and *t* factors were 0.00243 and -3.04722, respectively, indicating that both means cannot be viewed as different.

We have also studied the stability of the H2A.Bbd nucleosome variant at very low particle concentrations. Under these conditions, a selective release of the H2A–H2B dimer occurred, which reflects the disruption of the H2A–H2B dimer interactions with both the $(H3-H4)_2$ tetramer and DNA (Claudet *et al*, 2005). If the H2A.Bbd–H2B variant dimer exhibited lower stability relative to the conventional one, a release of H2A.Bbd–H2B dimer at higher nucleosome

Figure 1 (**A**) Microccocal nuclease digestion kinetics of conventional and H2A.Bbd nucleosomes. Identical amount of conventional nucleosomes (nuc H2A) and H2A.Bbd nucleosomes (nuc Bbd) were digested (in presence of 100 µg/ml plasmid DNA) with 8 U/ml of microccocal nuclease for the indicated times. The reaction was stopped by addition of 20 mM EDTA and 0.1 mg/ml proteinase K, 0.1% SDS. DNA was isolated and run on a 10% polyacrylamide gel. The lower panel shows the scans of the gel. 50 bp M, marker DNA fragments (the molecular mass of the fragments is indicated at the left part of the figure). (**B**, **C**) AFM imaging shows that the H2A.Bbd variant histone octamer organizes 127 bp of DNA. A 255 bp fragment containing the 601 positioning sequence and either conventional or H2A.Bbd variant octamers were used to reconstitute centrally positioned nucleosomes. Both types of nucleosomes were visualized by AFM. AFM images of conventional nucleosomes (nuc H2A) are presented in (B), and variant H2A.Bbd nucleosomes (nuc Bbd) are shown in (C). An enlarged view of a conventional or variant H2A.Bbd nucleosome particle is shown below the B and C panels. (**D**) Quantification of the data of (B) and (C). The measured mean length of the DNA in complex with the H2A.Bbd variant histone octamer was only 127 ± 2.2 bp compared to 146 ± 1.3 bp for conventional H2A nucleosomes. A color version of this figure is available at '*The EMBO Journal* online'.
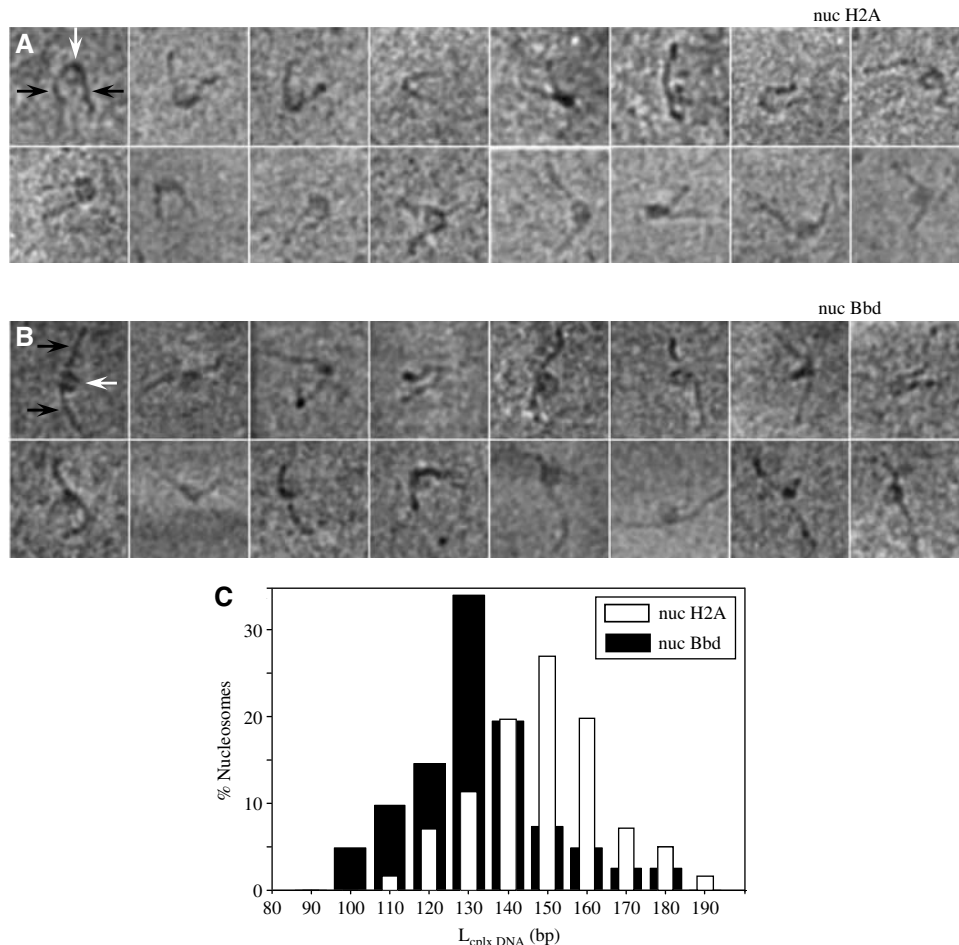
nuc H2A

nuc Bbd

Figure 2 Conventional and H2A.Bbd histone variant nucleosomes exhibit different organization of the entry and exit nucleosomal DNA ends. Centrally positioned conventional and H2A.Bbd variant nucleosomes were reconstituted on a 255 bp DNA fragment containing the 601 positioning sequence and visualized by cryo-EM. (**A**) Representative cryo-electron micrographs of conventional nucleosomes. The majority of the entry and exit DNA ends (black arrows) form a V-shaped structure with the nucleosome (designated with white arrow) localized in the center. (**B**) Same as (A) but for variant H2A.Bbd nucleosomes. The majority of the DNA ends (black arrows) form an angle close to 180°. (**C**) Quantification of the data of (A) and (B). The length of DNA (132 ± 2.6 bp) complexed with the H2A.Bbd variant octamer was essentially the same (within the margin of the experimental error) as that measured by AFM.

concentration would be expected. Figure 3C showed that this is indeed the case. At the lowest particle concentration studied (3.8 nM), the vast majority of the H2A.Bbd–H2B dimers was released from the variant H2A.Bbd particle (Figure 3C, the panel and the scan nuc Bbd-H3*) in contrast to conventional particle (Figure 3C, the panel and the nuc H2A-H3* scan). This showed that the interactions between the H2A.Bbd–H2B dimer with both (H3-H4)$_2$ tetramer and DNA within the H2A.Bbd particle were altered, which conferred lower stability to the H2A.Bbd variant nucleosomal particle.

SWI/SNF is unable to remodel nucleosome particles reconstituted with swapped tail H2A–H2A.Bbd mutants containing the H2A.Bbd histone fold domain

The H2A.Bbd particle exhibits distinct structural and functional properties, including an inability to be remodeled by SWI/SNF (Angelov *et al*, 2004). The mechanism and the role of different H2A.Bbd domains in this interference of the remodeling are not known. We approached this problem by studying the properties of nucleosomes containing H2A.Bbd–H2A swapped domain mutants. Initially, we have focused on

the N-terminal and C-terminal swapped-tail mutants (schematically depicted in Figure 4B). The different mutant proteins were purified (Figure 4C) and efficiently incorporated into nucleosomes (Figure 4D and E). The DNase I footprinting analysis showed that nucleosomes that contain the histone fold domain of H2A.Bbd, exhibited the same alterations in the DNase I digestion pattern as the H2A.Bbd nucleosome (Figure 4F, compare lanes 1, 2 and 4 with lanes 3 and 5), suggesting that this domain alone determines the perturbations observed in the structure of the H2A.Bbd nucleosome. To test whether SWI/SNF was able to remodel the swapped-tail mutants, which contain the histone-fold domain of H2A.Bbd, we used DNase I footprinting (Figure 5). The DNase I footprinting shows that SWI/SNF was able to remodel chimeric nucleosomes containing the histone fold domain of conventional H2A (lanes 1–4 and 13–16), but not the chimeric nucleosomes containing the histone fold domain of H2A.Bbd (lanes 5–12 and 17–20). Therefore, the presence of the histone fold domain of H2A.Bbd in a nucleosomal particle was sufficient to generate structural properties that prevent the remodeling by SWI/SNF.
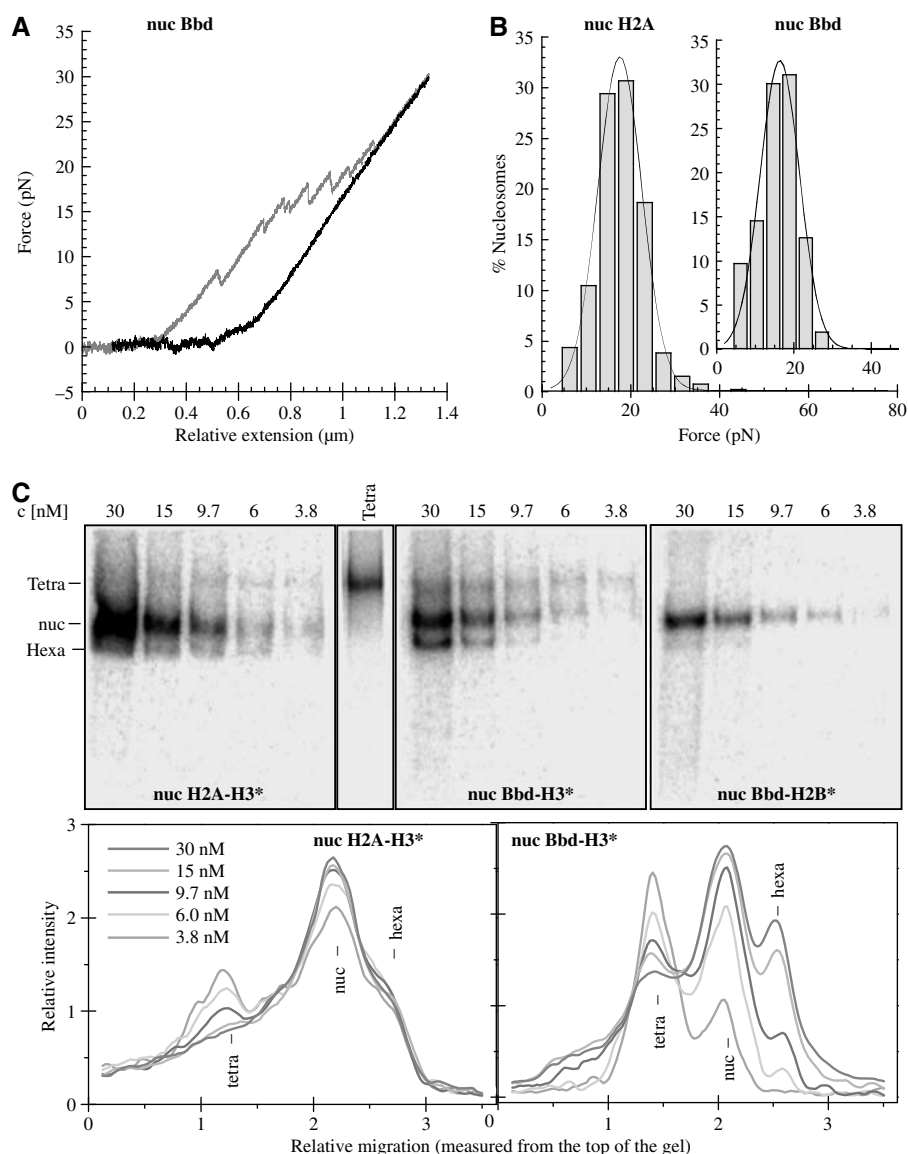
Figure 3 Force measurements of the disruption of a single variant H2A.Bbd nucleosome. Gel-purified 5S rDNA tandem repeats were labeled at one end with biotin-dCTP, whereas the other end was labeled with digoxigenin-dUTP. The fragments were used for reconstitution of nucleosomal arrays containing either conventional H2A or variant H2A.Bbd histones. One end of the DNA of an individual nucleosomal array was stuck on a digoxigenin functionalized bead, whereas the other was attached to a streptavidin functionalized bead. This individual nucleosomal arrays tethered between the two beads was stretched by using optical tweezers device. (**A**) Force–extension curve of the stretching cycle. The extension is shown in red (upper curve) whereas the relaxation is in black. Note the typical 'saw tooth' profile of the force extension curve. Each tooth reflects the disruption of a single H2A.Bbd particle or the simultaneous disruption of two particles. (**B**) Distribution profile of the disruption forces of a single H2A.Bbd particle (nuc Bbd) and conventional H2A particle (nuc H2A). (**C**) Stability of conventional and H2ABbd nucleosomes as a function of nucleosome concentration. End positioned nucleosomes were reconstituted on a 241 bp DNA fragment comprising the 601 sequence using either ^{32}P-labeled H3 (H3*) or ^{32}P-labeled H2B (H2B*). The tetrameric particles contained ^{32}P-labeled H3. The nucleosome solutions were diluted to the indicated concentrations and were run on a 5% native polyacrylamide gel. The positions of the nucleosomes and the tetrameric (H3–H4)$_2$ particles are indicated on the left part of the gel. The lower panel shows the scans of the gels for the conventional and H2A.Bbd variant nucleosomes containing ^{32}P-labeled H3. Because the amount of the loaded material on the different wells was different, the presented measured intensities were normalized to the concentration. A color version of the figure is available at '*The EMBO Journal* online'.

Involvement of the H2A.Bbd docking domain in the wrapping of nucleosomal DNA

The major difference between the conventional H2A and the histone variant H2A.Bbd is observed in the C-terminal domain of the two proteins. H2A.Bbd does not have the characteristic C-terminus of the H2A family and lacks the very end of the docking domain involved in the interaction with H3 in the nucleosome (Figure 4A and Bao *et al*, 2004). The fusion of C-terminal tail of H2A to H2A.Bbd was not sufficient to generate a nucleosomal particle, which can be remodeled by SWI/SNF (Figure 5, lanes 9–12), indicating that the absence of a C-terminal tail in H2A.Bbd is probably not responsible for the particular properties of this variant towards SWI/SNF remodeling. To test whether the divergent docking domain of H2A.Bbd could be involved in the generation of the specific properties of the H2A.Bbd nucleosome, we have produced and purified a H2A.Bbd mutant to homogeneity, in which the docking domain of H2A.Bbd was
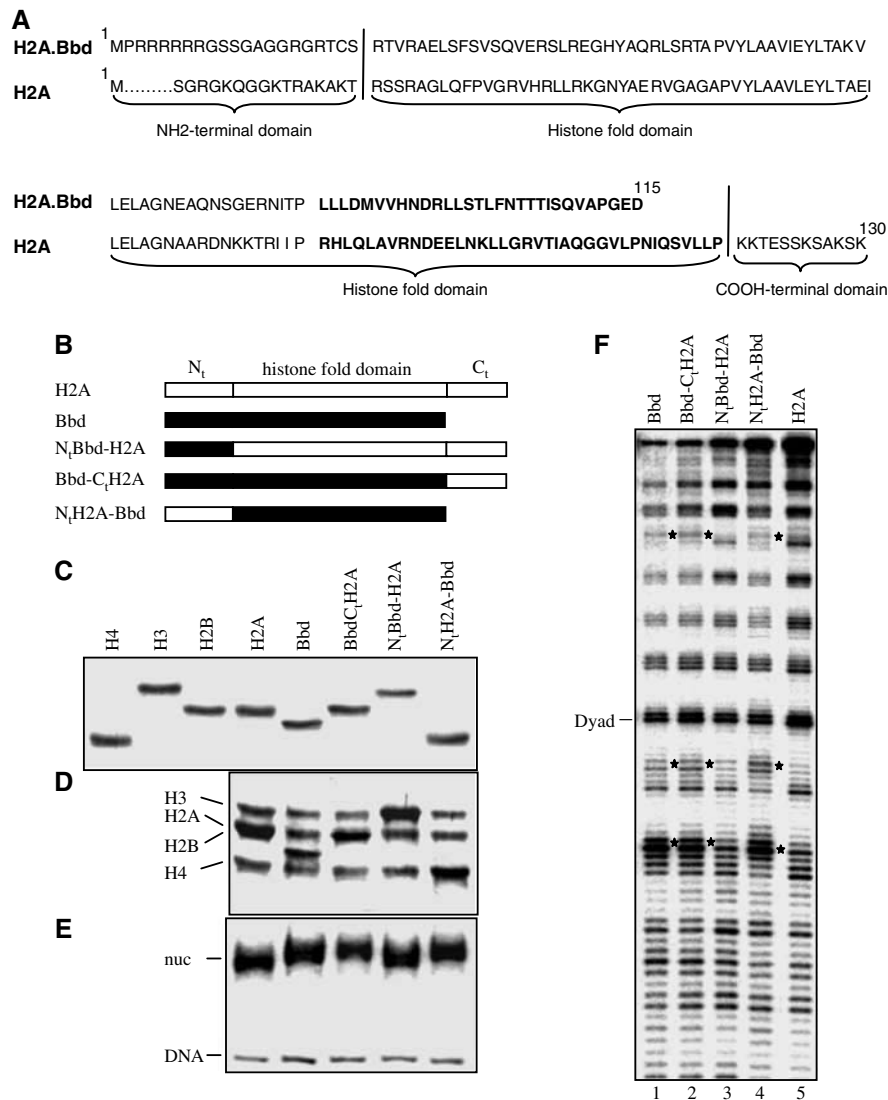
Figure 4 Biochemical characterization of the conventional H2A and H2A.Bbd nucleosomes swapped-tail mutants. Conventional core histones, H2A.Bbd (Bbd), swapped-tail Bbd-C$_t$H2A (a fusion between H2A.Bbd and the C-terminal domain of conventional H2A), N$_t$Bbd-H2A (a fusion of the N-terminus of H2A.Bbd and the histone fold and C-terminus of conventional H2A), N$_t$H2A-Bbd (a fusion of the N-terminus of H2A and the H2A.Bbd histone fold domain) and fragment of DNA containing the 154 bp DNA fragment of 5S gene, were used to reconstitute nucleosomes. (**A**) Sequence of H2A and H2A.Bbd proteins. The different domains of the protein are indicated in the figure. The docking domain is in bold. (**B**) Schematics of different proteins used for nucleosome reconstitution. (**C**) Eighteen percent SDS–PAGE of the purified recombinant core histones, H2ABbd and the swapped-tail histone mutants. (**D**) Histone composition of the reconstituted nucleosomes. The histones were separated on a 18% SDS–PAGE gel. The positions of the conventional core histones are designated. (**E**) EMSA analysis of the reconstituted nucleosomes. The positions of the nucleosomes (nuc) and the naked DNA are indicated on the left part of the figure. (**F**) DNase I footprinting of the reconstituted conventional H2A, variant H2A.Bbd and the swapped-tail histone mutant nucleosomes. Note that the presence of the histone fold domain of H2A.Bbd was sufficient to induce the DNAse I digestion characteristic of the H2A.Bbd alterations (indicated by stars).

replaced by both the docking domain and the C-terminal tail of conventional H2A (Bbd-ddH2A). This recombinant protein was used to reconstitute chimeric nucleosomes (Figure 6A). Subsequently, the structure of the Bbd-ddH2A nucleosomes was analyzed by DNase I footprinting (Figure 6B). Interestingly, the DNase I digestion pattern of the Bbd-ddH2A nucleosomes was almost the same as that of H2A.Bbd nucleosomes (with the characteristic alterations in DNAse I sensitivity) compared to conventional nucleosomes. This indicates that the presence of the docking domain of H2A was not sufficient to restore the DNAse I digestion pattern of conventional nucleosomes.

We next measured the length of DNA wrapped around the Bbd-ddH2A histone octamer by AFM. Interestingly, the length

of the DNA organized by the Bbd-ddH2A octamer was essentially the same (143 ± 2.2 bp) as for the conventional octamer (146 ± 1.3 bp) (Figure 6C). These measurements were statistically relevant, as a very significant number of nucleosomes (465 conventional and 208 Bbd-ddH2A) were used in these experiments. Therefore, the presence of the docking domain and the C-terminal tail of H2A in the Bbd-ddH2A nucleosome led to the wrapping of an additional 15 bp of DNA around the histone octamer.

We have also studied the conformation of the Bbd-ddH2A nucleosome in vitrified solution by cryo-EM (Figure 6D). The electron cryo-micrographs showed that the proportion of the Bbd-ddH2A nucleosomes exhibiting V-type structure (typical for the conventional H2A nucleosome) is definitely higher
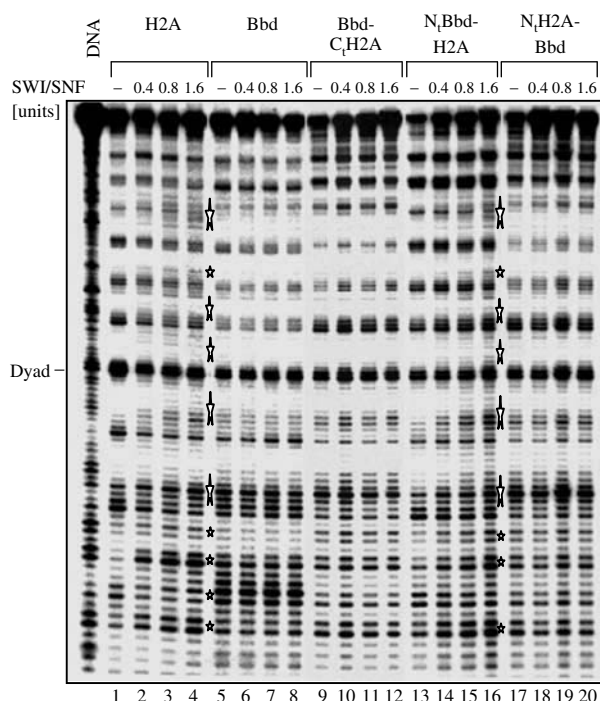
Figure 5 Remodeling of conventional H2A, variant H2A.Bbd and swapped-tail H2A and H2A.Bbd histone mutant nucleosomes. A 154 bp ^{32}P-end labeled DNA fragment comprising the 5S *Xenopus borealis* gene was used for reconstitution. The indicated increasing amounts of SWI/SNF were added to the nucleosome solutions and they were incubated at 30°C for 45 min in the presence of 1 mM ATP. The nucleosome remodeling was assessed by DNase I footprinting. Lanes 1, 5, 9, 13 and 17, DNase I footprinting of nucleosomes in the absence of SWI/SNF. Note that SWI/SNF was unable to remodel the nucleosomes, which contained the histone fold of H2ABbd. Stars indicate DNA fragments that appear after SWI/SNF remodeling.

compared to the parental H2A.Bbd nucleosomes (compare Figure 6D and Figure 2A with Figure 2B). We conclude that the docking and C-terminus domains of H2A were able to rescue the specific orientation of the entry/exit of nucleosomal DNA to a considerable extent, possibly by reducing the breathing of the nucleosomal DNA ends.

The docking domain and C-terminal tail of H2A partially restore the ability of SWI/SNF to remodel Bbd-ddH2A nucleosomes

The data described above show that nucleosome particle containing the Bbd-ddH2A chimeric protein exhibited physico-chemical properties similar, but not identical, to nucleosome containing the conventional H2A histone. This raises the question whether Bbd-ddH2A nucleosomes exhibit functional properties similar to H2A nucleosomes and in particular towards SWI/SNF induced mobilization, remodeling and nucleosomal particle stability. We first used AFM to monitor nucleosome mobilization (Figure 7A). Briefly, centrally positioned conventional, H2A.Bbd and Bbd-ddH2A nucleosomes were incubated with SWI/SNF in the presence or absence of ATP and then visualized by AFM. The percentage of nucleosomes centrally and end– positioned (respectively P_{cent} and P_{end}) were counted 'before' and 'after' the mobilization reaction. Then, the mobilization efficiency can be calculated by applying: $\%_{sliding} = P_{end}^{after} - P_{end}^{before}/P_{cent}^{before}$ (i.e. the percen-

tage of the effectively slided nucleosomes relatively to the proportion of initially centered nucleosomes). Under the experimental conditions, 52% of conventional H2A, 14% of H2A.Bbd and 31% of Bbd-ddH2A particles were mobilized by SWI/SNF in the presence of ATP, indicating that the presence of the docking domain and C-terminal tail of H2A in H2A.Bbd is able to rescue partially the ability of SWI/SNF to mobilize the nucleosomes. In addition, remodeling (Figure 7B) and stability (Figure 7C) of Bbd-ddH2A nucleosome particles were very similar to those of conventional nucleosomes. Indeed, SWI/SNF was able to remodel Bbd-ddH2A nucleosomes (Figure 7B) and the Bbd-ddH2A particles are more stable relative to the H2A.Bbd particles when subjected to dilution (compare Figure 7C with the panels of Figure 3C). This suggests that the stability and the nucleosomal DNA organization in H2A.Bbd nucleosomes are dependent on the docking domain of H2A.Bbd. The whole histone fold domain of H2A.Bbd is, however, responsible for the weaker mobilization of the H2A.Bbd nucleosome by SWI/SNF.

Discussion

In this paper, we have carried out a detailed analysis on the structural and functional properties of the H2A.Bbd nucleosome and dissected the role of its different domains using a combination of physical, biochemical and molecular biology approaches. AFM and cryo-EM were used to directly measure the length of the DNA wrapped around the variant histone octamer. Remarkably, both methods showed that 130 bp of DNA were wrapped around the H2A.Bbd histone octamer. This result is in complete agreement with our micrococcal nuclease digestion data, which showed a strong kinetics intermediate at 128 bp in the digestion profile of the variant H2A.Bbd particle (Figure 1A).

The EMSA experiments of nucleosomes at very low concentrations showed directly that the H2A.Bbd nucleosome was less stable compared to the conventional nucleosome and that the interaction of the H2A.Bbd–H2B dimer with the $(H3–H4)_2$ tetramer and nucleosomal DNA was weaker than that of the conventional H2A–H2B dimer, which is in agreement with the data on the measurements of the sedimentation coefficient of the H2A.Bbd particle (Gautier *et al*, 2004). Recent FRET experiments suggested that the nucleosomal ends of the H2A.Bbd particle were weakly bound to the histone octamer (Bao *et al*, 2004). Our data confirmed these results and in addition showed that the DNA ends are released from the surface of the H2A.Bbd octamer and no longer formed, as in the case of conventional nucleosome, a V-type structure. We hypothesized that ~10 bp of each end of nucleosomal DNA are released from their interactions with the histone octamer in the H2A.Bbd nucleosome. The optical tweezers elasticity measurements of the force, necessary for the unfolding of single H2A.Bbd nucleosome gave, however, very close value to the force required for the unfolding of a conventional H2A nucleosome (16.1 ± 4.8 versus 17.8 ± 5.3 pN). This could be explained by the thermodynamical considerations of Kulic and Schiessel (2004), which showed that in the stretching experiments the major part of the energy necessary for the nucleosome unfolding appeared to be absorbed by the flipping of the nucleosome around its dyad and only a small part is consumed by the unwrapping of the DNA from the histone octamer.
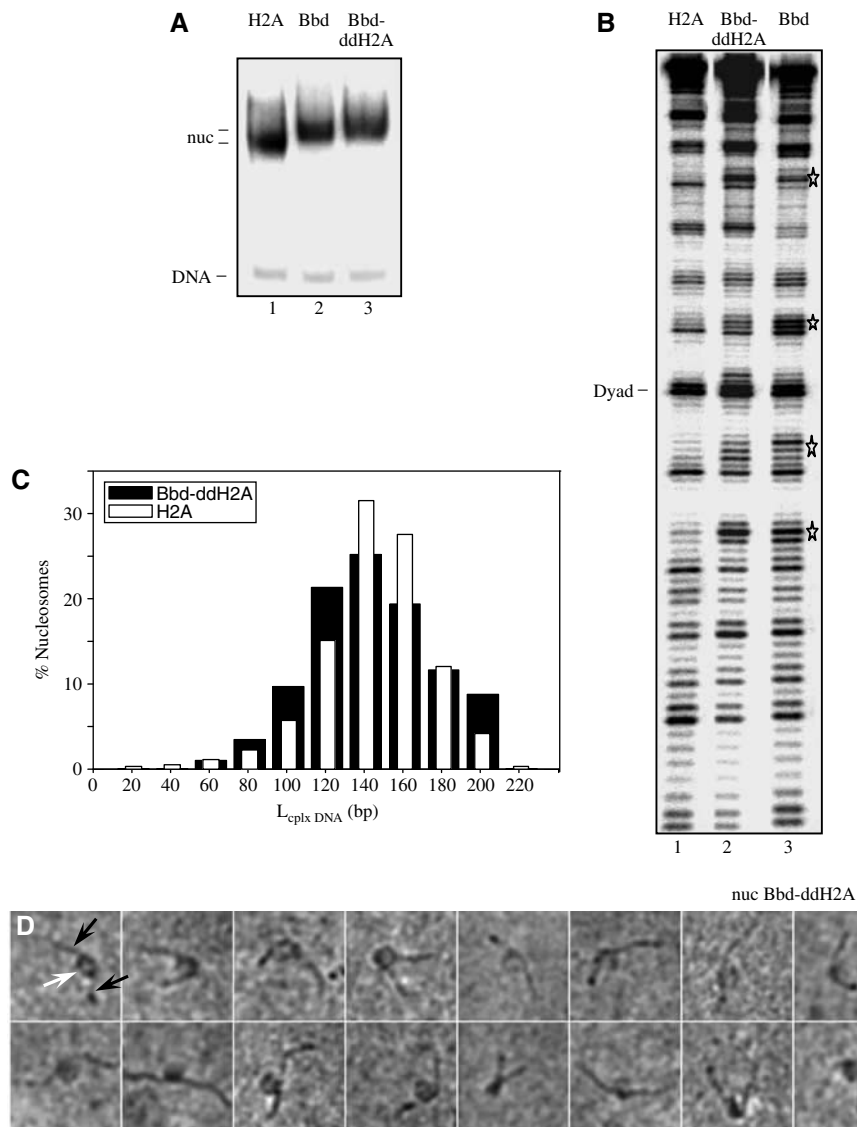
Figure 6 Characterization of nucleosomes reconstituted with the fusion of the histone fold (without the docking domain) of H2A.Bbd and the docking domain and the C-ter of H2A (Bbd-ddH2A). (**A**) EMSA of reconstituted nucleosomes. (**B**) DNase I footprinting of the reconstituted particle shown in (A). The stars indicate the altered DNase I digestion pattern of the H2A.Bbd and Bbd-ddH2A nucleosomes. (**C**) Distribution of the DNA in complex with the histones in conventional and Bbd-ddH2A nucleosomes. Conventional and Bbd-ddH2A nucleosomes were reconstituted on a 255 bp 601 DNA fragment and the particles were visualized by AFM. Note that both conventional and Bbd-ddH2A octamers organize the same length of DNA within the nucleosome. (**D**) Electron cryo-microscopic visualization of Bbd-ddH2A particles. A higher proportion of the particles exhibit, like the conventional H2A reconstituted nucleosome (see Figure 2A), a V-shaped structure; the black arrows designated the DNA ends, whereas the nucleosome is designated by white arrow.

SWI/SNF was not able to remodel the N- and C-terminal swapped tail H2A and H2A.Bbd mutants, indicating that the histone fold domain of H2A.Bbd, but not its peculiar N-terminus or the absence of C-terminal tail, determines this property of the H2A.Bbd particle (Figure 5). This could reflect the alterations in the structure of nucleosomes containing the histone fold domain of H2A.Bbd (Figure 4). The replacement of the docking domain of H2A.Bbd with that of H2A (Bbd-ddH2A) makes a fusion protein, which upon incorporation into the histone octamer, was able to generate a particle with some properties characteristic for the conventional H2A particle (Figures 6 and 7). For example, the length of the DNA organized by the histone octamer, the SWI/SNF-mediated remodeling and the *in vitro* stability of the nucleosomal particle containing the Bbd-ddH2A were very similar to

what was obtained with the particle containing the H2A protein. However, the DNase I footprinting assay revealed that the Bbd-ddH2A nucleosomal particles exhibited almost the same structural alterations as parental H2A.Bbd nucleosomes. In addition, incorporation of the fusion protein Bbd-ddH2A in nucleosomal particles led to an assembly of only a subset of particles with the V-type conformation characteristic for the conventional nucleosomes (Figures 2A and 6D) and to only a partial rescue of the efficiency of nucleosome mobilization by SWI/SNF (Figure 7A). All together, the data reported in this manuscript allowed us to conclude that the whole histone fold domain of H2A.Bbd determines its unusual structural and functional properties.

The *in vitro* transcription assays have shown that arrays containing H2A.Bbd nucleosomes were more easily tran-
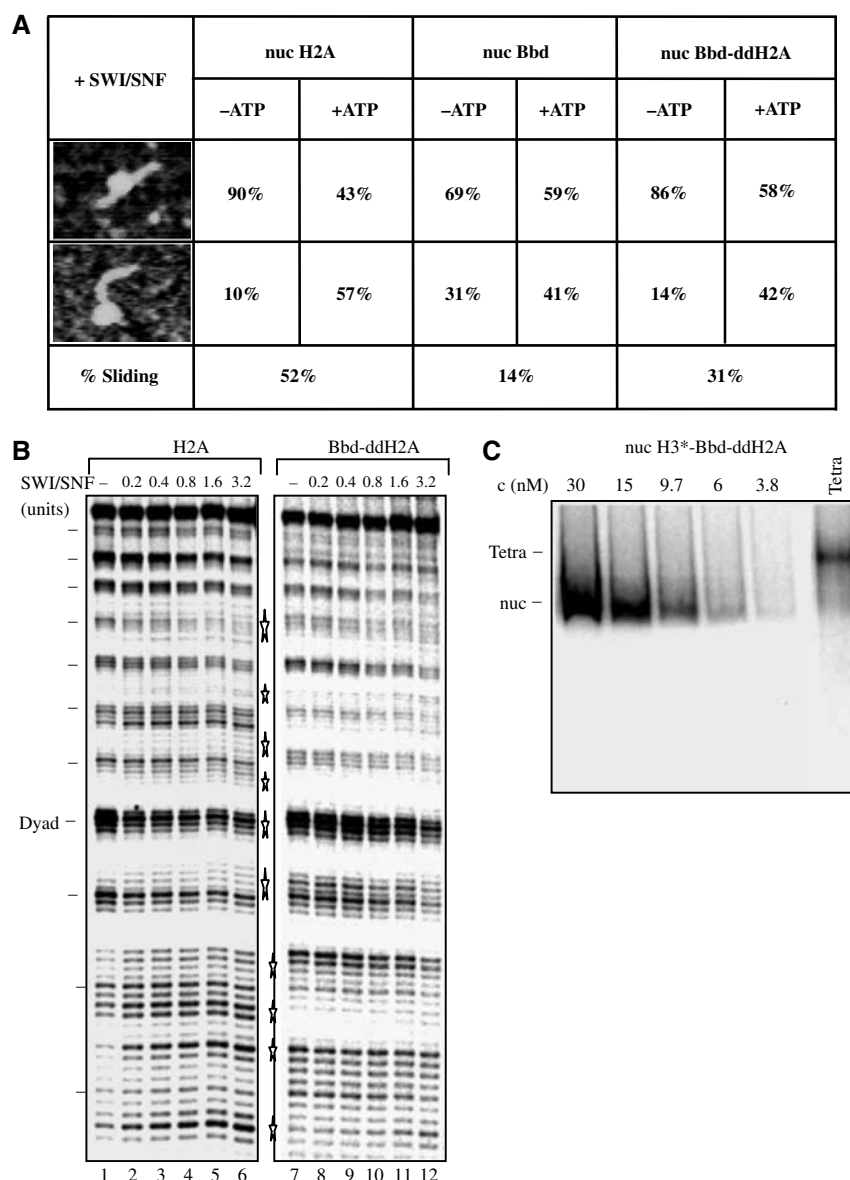
A

+ SWI/SNF	nuc H2A		nuc Bbd		nuc Bbd-ddH2A	
	–ATP	+ATP	–ATP	+ATP	–ATP	+ATP
	90%	43%	69%	59%	86%	58%
	10%	57%	31%	41%	14%	42%
% Sliding	52%		14%		31%	

Figure 7 The fusion of the docking domain of H2A to H2A.Bbd partially rescues the ability of SWI/SNF to remodel the nucleosomes. (**A**) Centrally positioned nucleosomes were reconstituted on a 255 bp DNA fragment containing the 601 sequence. SWI/SNF (1 unit) was added to the nucleosome solutions and they were incubated at 29°C for 60 min in the presence/absence of ATP, then the samples were visualized by AFM and the percentage of mobilized nucleosomes (% sliding in the figure) was calculated (see the text). The number of analyzed nucleosomes in absence and presence of ATP were 140 and 132 for nucH2A, 221 and 236 for nuc Bbd, 119 and 115 for nuc Bbd-ddH2A. (**B**) Nucleosome remodeling assessed by DNase I footprinting of conventional (lanes 1–6) and Bbd-ddH2A (lanes 7–12) nucleosomes. A 154 bp ^{32}P-end labeled DNA fragment comprising the 5S *X. borealis* gene was used for reconstitution. The indicated increasing amounts of SWI/SNF were added to the nucleosome solutions and they were incubated at 30°C for 45 min in the presence of 1 mM ATP. Lanes 1 and 7, DNase I footprinting in the absence of SWI/SNF. Stars indicate DNA fragments that appear after SWI/SNF remodeling. (**C**) Stability of Bbd-ddH2A nucleosomes as a function of nucleosome concentration. The experiments were carried out as in Figure 3 (see legend of Figure 3). The positions of the nucleosomes and the tetrameric $(H3-H4)_2$ particles are indicated on the left part of the gel.

scribed and acetylated than conventional H2A arrays (Angelov *et al*, 2004). In addition, H2A.Bbd was found to colocalize with acetylated H4 within the nucleus (Chadwick and Willard, 2001). These data suggest that, *in vivo*, the presence of H2A.Bbd could be viewed as a marker of active chromatin. The structural properties of H2A.Bbd nucleosomes described in this study as well as the previously reported data (Angelov *et al*, 2004; Gautier *et al*, 2004) point to a possible mechanism for the role of H2A.Bbd nucleosomes in the assembly and maintenance of transcriptionally active chromatin. The exchange of conventional H2A

with H2A.Bbd would create a more relaxed structure, which, in turn, would facilitate interaction of transcription factors, chromatin modifying enzymes and polymerases with H2A.Bbd chromatin allowing a more efficient transcription initiation as previously suggested (Angelov *et al*, 2004). Because the H2A.Bbd nucleosomes cannot be mobilized by the SWI-SNF and ACF machineries alone (Angelov *et al*, 2004) or in presence of histone chaperones (Angelov *et al*, 2006), the cell would not be able to use these chromatin remodelers to slide the histone octamers and to create nucleosome-free promoter regions. Instead, eviction of the histone octamers

should be used, a process which would be facilitated by the weaker stability of the H2A.Bbd nucleosomes.

Materials and methods

Preparation of DNA fragments

The 255 and 241 bp DNA fragments, containing the 601 nucleosome positioning sequence at the middle or at the end of the fragment, were obtained by polymerase chain reaction (PCR) amplification from plasmid pGem-3Z-601 and p199-1, respectively (kindly provided by B Bartholomew and J Widom). Labeling was performed by adding 30 µCi of [-^{32}P] CTP to the PCR reaction. The 207 bp 5S DNA fragment was obtained by PCR amplification from plasmid pXP-10. PCR product was digested with EcoRI and RsaI and the resulting 154 bp fragment was labeled at the 3'end by filling with dATP and [-^{32}P]dTTP. All labeled DNA fragments used for nucleosome reconstitution were gel purified.

For the stretching experiment, plasmid p2085S-G5E4, (kind gift from JL Workman) was digested with Acc65I, CaiI, SspI and ClaI. The restriction fragment containing the ~400 bp E4 promoter DNA, flanked by two DNA sequences, each composed of five 208 bp tandem repeats of the 5S rRNA sea urchin gene (Neely et al, 1999), was purified by 4% native polyacrylamide gel electrophoresis and end-labeled at the ClaI side by biotin-dCTP. A fraction of biotin-dCTP-labeled fragments was labeled at the Acc65I end by digoxigenin-dUTP. These DNA fragments, single or double labeled at both ends, were mixed at a ratio of 1:10 and used for reconstitution of conventional and H2A.Bbd nucleosomal arrays (Claudet et al, 2005). The attachment of the reconstituted arrays to the polystyrene beads was performed as described earlier (Claudet et al, 2005).

Protein purification, nucleosome reconstitution, remodeling and stability

Recombinant Xenopus laevis full-length histone proteins were produced in bacteria and purified as described (Luger et al, 1999). For the H2A.Bbd protein and its mutants, the coding sequences for the H2A and for H2A.Bbd were amplified by PCR and introduced in the pET3a vector. NtBbd-H2A (H2A.Bbd domain from M1 to S21 in frame to H2A domain from R18 to K130); Bbd-CtH2A (H2A.Bbd domain from M1 to D115 fused to H2A domain from T121 to K130); NtH2A-Bbd (H2A domain from M1 to T17 fused to H2A.Bbd domain from R22 to D115); Bbd-ddH2A (H2ABbd domain from M1 to I83 fused to H2A domain from P81 to K130); H2A-ddBbd (H2A domain from M1 to I80 fused to H2A.Bbd domain from T84 to D115). Recombinant proteins were purified as previously described (Angelov et al, 2004).

Yeast SWI/SNF complex was purified as described previously (Cote et al, 1994) and its activity was normalized by measuring its effect on the sliding of conventional nucleosomes: 1 unit being define as the amount of SWI/SNF required to mobilize 50% of input nucleosomes (50 ng) at 30°C during 45 min. Nucleosome reconstitution was performed by the salt dialysis procedure (Mutskov et al, 1998). Carrier DNA (150–200 bp, 2 µg) and 50 ng of ^{32}P-labeled DNA were mixed with equimolar amount of histone octamer in nucleosome reconstitution buffer NRB (2 M NaCl, 10 mM Tris pH 7.4, 1 mM EDTA, 5 mM MeEtOH). DNase I footprinting was performed as described previously (Angelov et al, 2003). Nucleosomes reconstituted on a 154 bp 5S DNA fragment (50 ng) were incubated with SWI/SNF as indicated in remodeling buffer containing 10 mM Tris–HCl, pH 7.4, 5% glycerol, 100 µg/ml BSA, 1 mM DTT, 0.02% NP40 40 mM NaCl, 2.5 mM MgCl$_2$ and 1 mM ATP for 45 min. The reaction was stopped by adding 1 µg of plasmid DNA, 0.02 U of apyrase, 10 mM EDTA.

Mobilization experiments were carried out using centrally positioned nucleosomes, reconstituted on a 255 bp DNA fragment containing the 601 positioning sequence. The nucleosome samples (5 ng/µl) were incubated in a solution of 10 mM Tris–HCl, pH 7.4, 1.5 mM MgCl$_2$ and 1 mM ATP for 60 min at 29°C.

Micrococcal nuclease digestion was performed at 8 U/ml at room temperature for indicated times in 10 mM Tris, pH 7.4, 1 mM DTT, 25 mM NaCl, 5% glycerol, 100 µg/ml BSA, 1.5 mM CaCl$_2$ and 100 µg/ml of plasmid carrier DNA. The digestion was stopped by adding 20 mM EDTA, 0.1% SDS, 200 µg/ml Proteinase K (30 min at 45°C). DNA was then extracted and run on a 10% native acrylamide-bisacrylamide (1/29 w/w) gel.

For the nucleosome dissociation experiments, a wild-type H3 and swapped tail H3–H2B mutant histones were used and labeled as previously described (Angelov et al, 2004). Nucleosome dissociation experiments were carried out in TE 10 mM NaCl. Briefly, aliquots of nucleosomes were diluted with the appropriate buffer in 10 µl final volume to the indicated concentrations (in the range of 30–3.8 nM), and left for 45 min at room temperature. Then the samples were analyzed by electrophoretic mobility shift assay (EMSA) on a 5% (w/v) polyacrylamide gel (acrylamide to bisacrylamide, 29:1 w/w), 0.3× TBE, at 4°C.

AFM, cryo-EM and optical tweezers

The cryo-EM analysis and stretching experiments were carried out essentially as described previously (Angelov et al, 2004; Claudet et al, 2005). For the AFM imaging, the conventional and variant nucleosomes were immobilized onto APTES-mica surfaces. The functionalization of freshly cleaved mica disks (muscovite mica, grade V-1, SPI) was obtained by self-assembly of a monolayer of APTES under argon atmosphere (Lyubchenko et al, 1993). Nucleosomes were filtered and concentrated using Microcon® centrifugal filters (DNA concentration ~75 ng/µl) to remove free histones from the solution, and diluted 10 times in Tris–HCl 10 mM, pH = 7.4, and 1 mM EDTA, just before deposition onto APTES-Mica surfaces. A 5-µl droplet of the nucleosome solution was applied on the surface for 1 min, rinsed with 1 ml of milliQ-Ultrapure© water and dried by spotting with an optic paper. The samples were visualized by using a Nanoscope III AFM (Digital Instruments™, Veeco, Santa Barbara, CA). The images were obtained in tapping mode in air, with silicon tips (resonant frequency 250–350 kHz) at scanning rates of 2 Hz over scan areas from 0.6 to 1 µm wide. The images (512 × 512 pixels) have been flattened using a homemade MATLAB© script to remove the long-term drift of the set-up. Complexed DNA length distribution was obtained by an automated analysis of AFM images using a home-written MATLAB© script allowing measuring the noncomplexed DNA length of each nucleosome. This program uses height and area criteria to segregate mononucleosomes from other objects in the image and morphological tools (such as erosion, dilatation and skeletonization) to measure their free DNA length. This type of analysis allows to partially overcome the tip convolution effect. Nucleosomes at the extreme position of the DNA fragment were excluded from the statistical analysis. The error on the distribution function mean value (standard error) is given by σ/N, where σ is the standard deviation of the experimental distribution and N is the number of analyzed nucleosomes (central limit theorem).

References

Abbott DW, Ivanova VS, Wang X, Bonner WM, Ausio J (2001) Characterization of the stability and folding of H2A.Z chromatin particles: implications for transcriptional activation. J Biol Chem **276:** 41945–41949

Ahmad K, Henikoff S (2002) Epigenetic consequences of nucleosome dynamics. Cell **111:** 281–284

Angelov D, Molla A, Perche PY, Hans F, Cote J, Khochbin S, Bouvet P, Dimitrov S (2003) The histone variant macroH2A interferes

with transcription factor binding and SWI/SNF nucleosome remodeling. *Mol Cell* **11:** 1033–1041

Angelov D, Bondarenko VA, Almagro S, Menoni H, Mongelard F, Hans F, Mietton F, Studitsky VM, Hamiche A, Dimitrov S, Bouvet P (2006) Nucleolin is a histone chaperone with FACT-like activity and assists remodeling of nucleosomes. *EMBO J* **25:** 1669–1679

Angelov D, Verdel A, An W, Bondarenko V, Hans F, Doyen CM, Studitsky VM, Hamiche A, Roeder RG, Bouvet P, Dimitrov S (2004) SWI/SNF remodeling and p300-dependent transcription of histone variant H2ABbd nucleosomal arrays. *EMBO J* **23:** 3815–3824

Ausio J, Abbott DW (2002) The many tales of a tail: carboxyl-terminal tail heterogeneity specializes histone H2A variants for defined chromatin function. *Biochemistry* **41:** 5945–5949

Bao Y, Konesky K, Park YJ, Rosu S, Dyer PN, Rangasamy D, Tremethick DJ, Laybourn PJ, Luger K (2004) Nucleosomes containing the histone variant H2A.Bbd organize only 118 base pairs of DNA. *EMBO J* **23:** 3314–3324

Bassing CH, Suh H, Ferguson DO, Chua KF, Manis J, Eckersdorff M, Gleason M, Bronson R, Lee C, Alt FW (2003) Histone H2AX: a dosage-dependent suppressor of oncogenic translocations and tumors. *Cell* **114:** 359–370

Beato M, Eisfeld K (1997) Transcription factor access to chromatin. *Nucleic Acids Res* **25:** 3559–3563

Becker PB (2002) Nucleosome sliding: facts and fiction. *EMBO J* **21:** 4749–4753

Bednar J, Horowitz RA, Dubochet J, Woodcock CL (1995) Chromatin conformation and salt-induced compaction: three-dimensional structural information from cryoelectron microscopy. *J Cell Biol* **131:** 1365–1376

Bednar J, Woodcock CL (1999) Cryoelectron microscopic analysis of nucleosomes and chromatin. *Methods Enzymol* **304:** 191–213

Celeste A, Difilippantonio S, Difilippantonio MJ, Fernandez-Capetillo O, Pilch DR, Sedelnikova OA, Eckhaus M, Ried T, Bonner WM, Nussenzweig A (2003) H2AX haploinsufficiency modifies genomic stability and tumor susceptibility. *Cell* **114:** 371–383

Chadwick BP, Valley CM, Willard HF (2001) Histone variant macroH2A contains two distinct macrochromatin domains capable of directing macroH2A to the inactive X chromosome. *Nucleic Acids Res* **29:** 2699–2705

Chadwick BP, Willard HF (2001) A novel chromatin protein, distantly related to histone H2A, is largely excluded from the inactive X chromosome. *J Cell Biol* **152:** 375–384

Claudet C, Angelov D, Bouvet P, Dimitrov S, Bednar J (2005) Histone octamer instability under single molecule experiment conditions. *J Biol Chem* **280:** 19958–19965

Costanzi C, Pehrson JR (1998) Histone macroH2A1 is concentrated in the inactive X chromosome of female mammals. *Nature* **393:** 599–601

Costanzi C, Pehrson JR (2001) macroH2A2, a new member of the macroH2A core histone family. *J Biol Chem* **276:** 21776–21784

Cote J, Quinn J, Workman JL, Peterson CL (1994) Stimulation of GAL4 derivative binding to nucleosomal DNA by the yeast SWI/SNF complex. *Science* **265:** 53–60

Dhillon N, Kamakaka RT (2000) A histone variant, Htz1p, and a Sir1p-like protein, Esc2p, mediate silencing at HMR. *Mol Cell* **6:** 769–780

Doyen CM, An W, Angelov D, Bondarenko V, Mietton F, Studitsky VM, Hamiche A, Roeder RG, Bouvet P, Dimitrov S (2006) Mechanism of polymerase II transcription repression by the histone variant macroH2A. *Mol Cell Biol* **26:** 1156–1164

Faast R, Thonglairoam V, Schulz TC, Beall J, Wells JR, Taylor H, Matthaei K, Rathjen PD, Tremethick DJ, Lyons I (2001) Histone variant H2A.Z is required for early mammalian development. *Curr Biol* **11:** 1183–1187

Gautier T, Abbott DW, Molla A, Verdel A, Ausio J, Dimitrov S (2004) Histone variant H2ABbd confers lower stability to the nucleosome. *EMBO Rep* **5:** 715–720

Henikoff S, Ahmad K (2005) Assembly of variant histones into chromatin. *Annu Rev Cell Dev Biol* **21:** 133–153

Henikoff S, Furuyama T, Ahmad K (2004) Histone variants, nucleosome assembly and epigenetic inheritance. *Trends Genet* **20:** 320–326

Kamakaka RT, Biggins S (2005) Histone variants: deviants? *Genes Dev* **19:** 295–310

Karras GI, Kustatscher G, Buhecha HR, Allen MD, Pugieux C, Sait F, Bycroft M, Ladurner AG (2005) The macro domain is an ADP-ribose binding module. *EMBO J* **24:** 1911–1920

Kulic IM, Schiessel H (2004) DNA spools under tension. *Phys Rev Lett* **92:** 228101

Kustatscher G, Hothorn M, Pugieux C, Scheffzek K, Ladurner AG (2005) Splicing regulates NAD metabolite binding to histone macroH2A. *Nat Struct Mol Biol* **12:** 624–625

Luger K, Mader AW, Richmond RK, Sargent DF, Richmond TJ (1997) Crystal structure of the nucleosome core particle at 2.8 A resolution. *Nature* **389:** 251–260

Luger K, Rechsteiner TJ, Richmond TJ (1999) Expression and purification of recombinant histones and nucleosome reconstitution. *Methods Mol Biol* **119:** 1–16

Lyubchenko YL, Oden PI, Lampner D, Lindsay SM, Dunker KA (1993) Atomic force microscopy of DNA and bacteriophage in air, water and propanol: the role of adhesion forces. *Nucleic Acids Res* **21:** 1117–1123

Mermoud JE, Costanzi C, Pehrson JR, Brockdorff N (1999) Histone macroH2A1.2 relocates to the inactive X chromosome after initiation and propagation of X-inactivation. *J Cell Biol* **147:** 1399–1408

Mutskov V, Gerber D, Angelov D, Ausio J, Workman J, Dimitrov S (1998) Persistent interactions of core histone tails with nucleosomal DNA following acetylation and transcription factor binding. *Mol Cell Biol* **18:** 6293–6304

Neely KE, Hassan AH, Wallberg AE, Steger DJ, Cairns BR, Wright AP, Workman JL (1999) Activation domain-mediated targeting of the SWI/SNF complex to promoters stimulates transcription from nucleosome arrays. *Mol Cell* **4:** 649–655

Pehrson JR, Fried VA (1992) MacroH2A, a core histone containing a large nonhistone region. *Science* **257:** 1398–1400

Perche PY, Vourc'h C, Konecny L, Souchier C, Robert-Nicoud M, Dimitrov S, Khochbin S (2000) Higher concentrations of histone macroH2A in the Barr body are correlated with higher nucleosome density. *Curr Biol* **10:** 1531–1534

Rangasamy D, Greaves I, Tremethick DJ (2004) RNA interference demonstrates a novel role for H2A.Z in chromosome segregation. *Nat Struct Mol Biol* **11:** 650–655

Redon C, Pilch D, Rogakou E, Sedelnikova O, Newrock K, Bonner W (2002) Histone H2A variants H2AX and H2AZ. *Curr Opin Genet Dev* **12:** 162–169

Rogakou EP, Pilch DR, Orr AH, Ivanova VS, Bonner WM (1998) DNA double-stranded breaks induce histone H2AX phosphorylation on serine 139. *J Biol Chem* **273:** 5858–5868

Santisteban MS, Kalashnikova T, Smith MM (2000) Histone H2A.Z regulates transcription and is partially redundant with nucleosome remodeling complexes. *Cell* **103:** 411–422

Sarma K, Reinberg D (2005) Histone variants meet their match. *Nat Rev Mol Cell Biol* **6:** 139–149

Strahl BD, Allis CD (2000) The language of covalent histone modifications. *Nature* **403:** 41–45

Suto RK, Clarkson MJ, Tremethick DJ, Luger K (2000) Crystal structure of a nucleosome core particle containing the variant histone H2A. Z *Nat Struct Biol* **7:** 1121–1124

Tsanev R, Russev G, Pashev I, Zlatanova J (1993) *Replication and Transcription of Chromatin*. Boca Raton, FL: CRC Press

van Holde KE (1980) DNA–histone interactions in nucleosomes. *Biophys J* **32:** 271–282

van Holde KE (1988) *Chromatin*. Berlin, Germany: Springer-Verlag KG